



ARTICLE

Genetics and Genomics

Pre-B acute lymphoblastic leukaemia recurrent fusion, *EP300-ZNF384*, is associated with a distinct gene expression

Barbara J. McClure^{1,2}, Susan L. Heatley^{1,2}, Chung H Kok^{1,2}, Teresa Sadras^{1,2}, Jiyuan An¹, Timothy P. Hughes^{1,2,3}, Richard B. Lock^{4,5}, David Yeung^{1,2,3}, Rosemary Sutton^{4,5,6} and Deborah L White^{1,2,6,7}

BACKGROUND: Zinc-finger protein 384 (*ZNF384*) fusions are an emerging subtype of precursor B-cell acute lymphoblastic leukaemia (pre-B-ALL) and here we further characterised their prevalence, survival outcomes and transcriptome.

METHODS: Bone marrow mononuclear cells from 274 *BCR-ABL1*-negative pre-B-ALL patients were immunophenotyped and transcriptome molecularly characterised. Transcriptomic data was analysed by principal component analysis and gene-set enrichment analysis to identify gene and pathway expression changes.

RESULTS: We exclusively detect E1A-associated protein p300 (*EP300*)-*ZNF384* in 5.7% of *BCR-ABL1*-negative adolescent/young adult (AYA)/adult pre-B-ALL patients. *EP300-ZNF384* patients do not appear to be a high-risk subgroup. Transcriptomic analysis revealed that *EP300-ZNF384* samples have a distinct gene expression profile that results in the up-regulation of Janus kinase/signal transducers and activators of transcription (JAK/STAT) and cell adhesion pathways and down-regulation of cell cycle and DNA repair pathways.

CONCLUSIONS: Importantly, this report contributes to a better overview of the incidence of *EP300-ZNF384* patients and show that they have a distinct gene signature with concurrent up-regulation of JAK-STAT pathway, reduced expression of B-cell regulators and reduced DNA repair capacity.

British Journal of Cancer (2018) 118:1000–1004; <https://doi.org/10.1038/s41416-018-0022-0>

INTRODUCTION

Many genomic lesions in precursor B-cell acute lymphoblastic leukaemia (pre-B-ALL) are associated with alterations of cytokine receptors or their signalling pathway mediators, transcription factors or regulators of differentiation.^{1,2} These lesions have prognostic significance, for example, *ETV6-RUNX1* is associated with a relatively favourable outcome compared with poor-risk disease associated with *BCR-ABL+* (Philadelphia-positive (Ph+)) or Ph-like ALL. Recently, next-generation sequencing studies have identified novel recurrent pre-B-ALL genomic lesions in genes such as *ABL1/2*, *JAK2*, *ZNF384*, *MEF2D* and *DUX4*,^{3,4} though the incidence and prognostic significance for some of these lesions are yet to be confirmed.

The E1A-associated protein p300 (*EP300*)-*ZNF384* fusion was initially reported as a recurrent fusion in 2015 with an incidence of 1.5% of paediatric B-ALL cases.⁵ Three additional studies have confirmed low incidence in paediatric populations (Supplementary Table 1), while adolescent and adult patients have a higher frequency.^{3,6} The *EP300* gene encodes a histone acetyltransferase (HAT), which influences transcription through chromatin remodeling and has tumour suppressor activity.⁷ The 3' fusion partner zinc-finger protein 384 (*ZNF384*) encodes a C2H2-type protein that plays a role in transcription and nucleocytoplasmic transport. How

EP300-ZNF384 fusion protein expression alters gene transcription to promote leukaemic cell growth and survival is only beginning to emerge.^{3,6,8}

In addition to *EP300*, multiple 5' fusion partners of *ZNF384* have been reported in lymphoproliferative disorders including *TAF15*,^{9,10} *ESWR1*,^{9,10} *CREBBP*,⁶ *TCF3*,^{6,9} *ARID1B*,⁹ *SYNRG*³ and *BMP2K*,¹¹ implying that *ZNF384* is the predominant pathogenic lesion. *ZNF384* and the majority of its fusion partners are located within close proximity to the telomeres of their respective chromosome, making the identification of *ZNF384* fusions difficult by conventional G-banding.^{5,9}

Given the increasing importance of *ZNF384* as a recurrent genetic lesion in pre-B-ALL, we examined its frequency and prognostic significance in our cohort of 274 *BCR-ABL1*-negative pre-B-ALL patients on which we have transcriptomic sequencing data.

MATERIALS AND METHODS

We studied 274 *BCR-ABL1*-negative pre-B-ALL patients (152 children, 54 adolescent/young adults (AYA, 16–39 years) and 68 adults) from the patient pool referred to us for Ph-like testing. Informed consent was obtained from each patient and the study

¹Cancer Theme, South Australian Health and Medical Research Institute (SAHMRI), Adelaide, SA 5000, Australia; ²School of Medicine, University of Adelaide, Adelaide, SA 5000, Australia; ³Haematology Department, SA Pathology, Adelaide, SA 5000, Australia; ⁴Children's Cancer Institute, Lowy Cancer Research Centre, University of New South Wales, Sydney, NSW 2000, Australia; ⁵School of Women's and Children's Health, University of New South Wales, Sydney, NSW 2000, Australia; ⁶Australian Genomics Health Alliance (AGHA), Murdoch Children's Research Institute, Parkville, VIC 3052, Australia and ⁷School of Paediatrics, University of Adelaide, Adelaide, SA 5000, Australia
Correspondence: Deborah L. White (deborah.white@sahmri.com)

Received: 7 September 2017 Revised: 22 December 2017 Accepted: 18 January 2018
Published online: 13 March 2018

was approved by the relevant institutional review board (Royal Adelaide Hospital Ethics Committee) and conducted in accordance with the Declaration of Helsinki. Transcriptomic sequencing data was generated using either Illumina HiSeq 2000 or NextSeq 500 platforms. Fusions and variants were identified (detail in Supplementary methods) and confirmed by reverse transcription polymerase chain reaction and Sanger sequencing. Samples were evaluated for a Ph-like signature by Taqman low-density array as previously described.¹²

For gene expression analysis, the raw fastq data was aligned by STAR aligner¹³ (version 2.4.2a) with two-pass method and described in full in the Supplementary methods, and only genes with false discovery rate (FDR) $p < 0.05$ were considered as statistically significant. Gene-set enrichment analysis (GSEA) was performed using Broad Institute GSEA software version 3.0 and Molecular Signature Database (MSigDB) version 5.2 (details are provided in Supplementary methods).

Five-year survival analysis of outcome data were estimated by Kaplan–Meier and log-rank test was used for significant difference, and we included Ph+ ALL cases for comparison. As part of our standard characterisation, immunophenotypic analysis was also performed for CD10, CD19 and CD34 expression.

RESULTS

Transcriptomic sequencing revealed 7/122 (5.7%) AYA/adult and 2/152 (1.3%) children harboured the *EP300-ZNF384* fusion gene (patient details Table 1). One additional paediatric patient harboured a *TCF3-ZNF384* fusion. In 7/9 patients the *EP300-ZNF384* fusion was detected at diagnosis, and in the one patient where matched diagnosis and relapse samples were available, the fusion was detected in both. In the remaining two patients only the relapse sample was available for study. Patients with *EP300-ZNF384* fusions did not express a Ph-like gene signature. Eight of nine patients had identical break points at *EP300* exon 6 (22q13) and *ZNF384* exon 3 (12p13) (Fig. 1a), with the remaining patient having a *ZNF384* breakpoint in exon 2. The resulting truncation of *EP300* eliminates the HAT and bromodomain, which reportedly reduces HAT activity and binding of acetylated proteins.⁸ In contrast to other studies that report multiple upstream *ZNF384* fusion partners,^{3,6,8} we identified predominantly *EP300-ZNF384* fusions in our cohort.

The patients harbouring *EP300-ZNF384* fusions had a median age of 24.5 years (range 4.4–47 years). In mononuclear cells (MNCs) of patients with *EP300-ZNF384* fusion ($n = 8$ available), the expression of CD10 was significantly lower when compared with other pre-B-ALL MNC ($n = 48$) ($p = 0.046$) (Fig. 1b). Surface expression of CD19 and CD34 was not significantly different between *EP300-ZNF384* ($n = 7$) and other pre-B-ALL groups ($p = 0.7882$ and $p = 0.1916$, respectively) (Fig. 1b). Of the five *EP300-ZNF384* patients where CD33 expression was available all had high expression.

Outcome data was available from 93 patients in our cohort (8 *EP300-ZNF384* patients, 24 Ph-like and 61 other pre-B-ALL). The 5-year survival of our cohort was 28.8%, with an average survival of 2.14 years. The notable poor survival seen in our AYA/adult pre-B-ALL cohort may reflect the inclusion of historical samples. Patients harbouring an *EP300-ZNF384* fusion had a 62.5% survival ($n = 8$) at 5 years. Outcomes for *EP300-ZNF384* patients compared favourably to other pre-B-ALL patients (27.2% 5-year survival; $n = 61$; $p = 0.083$) and Ph-like ALL patients¹⁴ (10.3% 5-year survival, $n = 24$; $p = 0.019$) (Fig. 1c), noting that four of the eight *EP300-ZNF384* patients were transplanted. For reference, we also included outcomes for 27 Ph+ ALL patients, the majority of whom were treated with tyrosine kinase inhibitor and chemotherapy, which had a 5-year survival of 40.3%.

Using transcriptomic sequencing, a variety of somatic variants were identified in *EP300-ZNF384* patients who are known to lead

to missense alterations in transcription factors, cytokine receptors and signalling pathways in key cancer driver genes (Table 1). At least one variant was detected in each *EP300-ZNF384* case, including RAS mutations in three (33.3%) patients, NRAS G12C and Q61P, and KRAS T58I. Two (22.2%) patients had a RUNX1 mutation, E111K ($n = 1$) and L29S ($n = 1$). Mutations were also detected in the FLT3 signalling axis in two patients (22.2%), FLT3 Y589H ($n = 1$) and FLT3LG R216H ($n = 1$). Three patients (33.3%) had cytokine receptor mutations including EPOR P488S ($n = 1$) or N487S ($n = 1$) and CSF1R N255I ($n = 1$).

To identify how gene expression is altered when the *EP300-ZNF384* is expressed, we then compared the transcriptomic analysis of eight AYA/adult *EP300-ZNF384* cases to eight non-*EP300-ZNF384* cases matched for age, initial white cell count and sex (patient details Supplementary Table 2). Unsupervised analysis using multidimensional scale (MDS) revealed that the *EP300-ZNF384* patient samples have a distinct gene expression profile compared to matched controls (Fig. 1d, Supplementary Figure 1). Gene expression analysis revealed differential expression of 984 genes (FDR $p < 0.05$) with similar numbers of genes up-regulated (476/984) or down-regulated (508/984). The heatmap (Fig. 1e) shows the differential gene expression based on the top 100 genes that discriminated between the two groups (Supplementary Table 3). Within the *EP300-ZNF384* cohort, up-regulation of *CLCF1* ($p < 0.001$), *CREB5* ($p < 0.001$), *STGALNAC2* ($p < 0.001$), *CD33* ($p < 0.001$) and *RUNX2* ($p < 0.001$) was observed and strong down-regulation of *OVCH2* ($p < 0.001$), *ARPP21* ($p < 0.001$), *NPY* ($p < 0.001$) and *BMP2* ($p < 0.001$). Expression of B-cell development regulators *PAX5* ($p = 0.03$), *IRF4* ($p = 0.004$) and *VPREB1* ($p < 0.0001$) were also significantly reduced in the *EP300-ZNF384* cohort. Altered regulation of myeloid reprogramming genes *GATA3*, *CEBPA* or *CEBPB* previously reported for this subgroup were not observed.⁶ Of note, the transcription factor, *KLF4*, which interacts with, and is acetylated by, EP300¹⁵ and negatively regulates PI3K signalling, was significantly down-regulated (log FC = -4.69 , $p < 0.001$) in the *EP300-ZNF384* patients. *KLF4* mediates TP53 action to regulate the G1–S phase transition following DNA damage. *TP53* expression was reduced by 1.98 fold in *EP300-ZNF384* patients compared to non-*EP300-ZNF384* patients ($n = 8$, $p = 0.0141$).

GSEA of our transcriptomic data showed that expression of *EP300-ZNF384* results in the up-regulation of genes related to Janus kinase/signal transducers and activators of transcription (JAK/STAT) signalling, leukocyte adhesion and differentiation pathways, whereas pathways related to cell cycle, oxidative phosphorylation and DNA repair are reduced (FDR $q < 0.05$) (Fig. 1f). GSEA analysis also revealed enrichment of genes containing motifs for LMO2 (FDR $q = 0.016$), RUNX1 (FDR $q = 0.014$) and GATA1 (FDR $q = 0.012$), all targets for ZNF384 interaction, and key regulators of haematopoiesis, and reduced expression from genes containing motifs for RB-1 (FDR $q = 0.000$).

The down-regulation of both *TP53* and *KLF4* in *EP300-ZNF384* samples may facilitate premature S phase entry prior to completion of DNA repair. This together with dampened EP300 acetylation function, a known modulator of TP53, may reduce genomic integrity¹⁶ and increase the potential for mutation acquisition in a setting of up-regulated JAK-STAT pathways and thus potentiate leukaemogenesis. *EP300-ZNF384* samples have reduced expression of both DNA repair reactome and DNA damage and repair pathways (Fig. 1f), suggesting that *EP300-ZNF384* expression contributes to higher genomic instability. Mutations or deletion of *TP53* are infrequent in pre-B-ALL but are common in many other tumours, and our transcriptomic data suggest that the down-regulation of DNA repair, relative to non-*EP300-ZNF384* pre-B-ALL, is an important feature of this cohort.

Table 1. Clinical findings and cytogenetic features of pre-B-ALL patients with ZNF384 fusions

Patient	Sex	Event	Fusion	Age at event	Initial WBC 10 ⁹ /ml	Initial CNS	Treatment	Karyotype	Variants	Outcome	Survival post Dx (years)
CH_A5049	M	Rel	TCF3-ZNF384	11.6		No data	ALLR3 therapy	47,XY,der(2)t(2:3)(p13;p21)t(2:7)(q33;q36),der(3)t(3)(p13;p21),der(7)t(q33;q36),+8[6]/46,XY[118]		Alive	5.9
CH_A1498	M	Rel	EP300-ZNF384	16.6		No data	ALLR3 therapy	46,XY,t(2:17)(q13;q11.2),del(6)(?q15q23)[7]/46,XY[13]	RUNX1 E111K	Alive	17.1
CH_A2973	M	Rel	EP300-ZNF384	17.1	11	No data	ANZCHOG ALL8 therapy	46,XY,der(7) del(7)(q?)inv(7)(q?) [12] /46,XY [7]	FLT3 Y589H	Died	4.4
AYAL_0004	M	Dx	EP300-ZNF384	16		No data	Study8	46,XY	KRAS T58I	Alive	6.9
AYAL_0004	M	Rel	EP300-ZNF384	23	2.58	Clear	Study8	45,X,-Y,t(1;12:6)(p36.1;q24.?)p21,t(2:9)(q11.2;q172),del(19)(p13)[14]/46,XY[21]		Alive	
AYAIL_0009	M	Dx	EP300-ZNF384	21	4.8	Clear	ALL6	45,XY,t(2:1)(p2?1;p15),del(6)(q13q273),inc[cp4]/46,XY[32],nuc.ish(TCF3x2)[200],(D4Z1,D10Z1,D17Z1)x2 [200],(ABL,BCR)x2[200],(ABL,BCR)x2[200],(MLL)x2 [200],(ETV6,RUNX1)x2[200]	NF1 Y1763F FLT3LG R216H	Alive	3.05
AYAIL_0021	F	Dx	EP300-ZNF384	28	5.4	Clear	LALA	t(X;14)	NRAS Q61P PTK2B G414V ETV6 L201P EPOR N487S	Died	1.81
AYAIL_0045	M	Dx	EP300-ZNF384	22	77.1	No data	ALSG	46,XY	CSFR1 N255I RUNX1 L29S	Died	11.63
ADI_0002	M	Dx	EP300-ZNF384	42		No data		46,XY	PTPN11 G60A		
ADI_0098	F	Dx	EP300-ZNF384	47	7.5	Clear	Hoeltzer	No data available	SH2B3 L6P EPOR P488S	Died	0.17
ADI_0159	F	Dx	EP300-ZNF384	43	25	No data		46,XX,t(13;14)(q14;q22)[11]/46,idem,t(12;22)(p13;q13)[4]/46,XX[45],ish 12p13(ETV6x2)[20],t(12;22)(WCP22+-WCP22-)[2/6],nuc ish(MYC,MLL,IGH)x2 [100],(ASSx1,ABL1x1,BCRx2)[90/100]	NRAS G12C	Died	2.76

pre-B-ALL precursor B-cell acute lymphoblastic leukaemia, LALA Leucémies Aiguës Lymphoblastiques de l'Adulte, ZNF384 zinc-finger protein 384, WBC white blood cell, CNS central nervous system, Dx diagnosis, Rel relapse

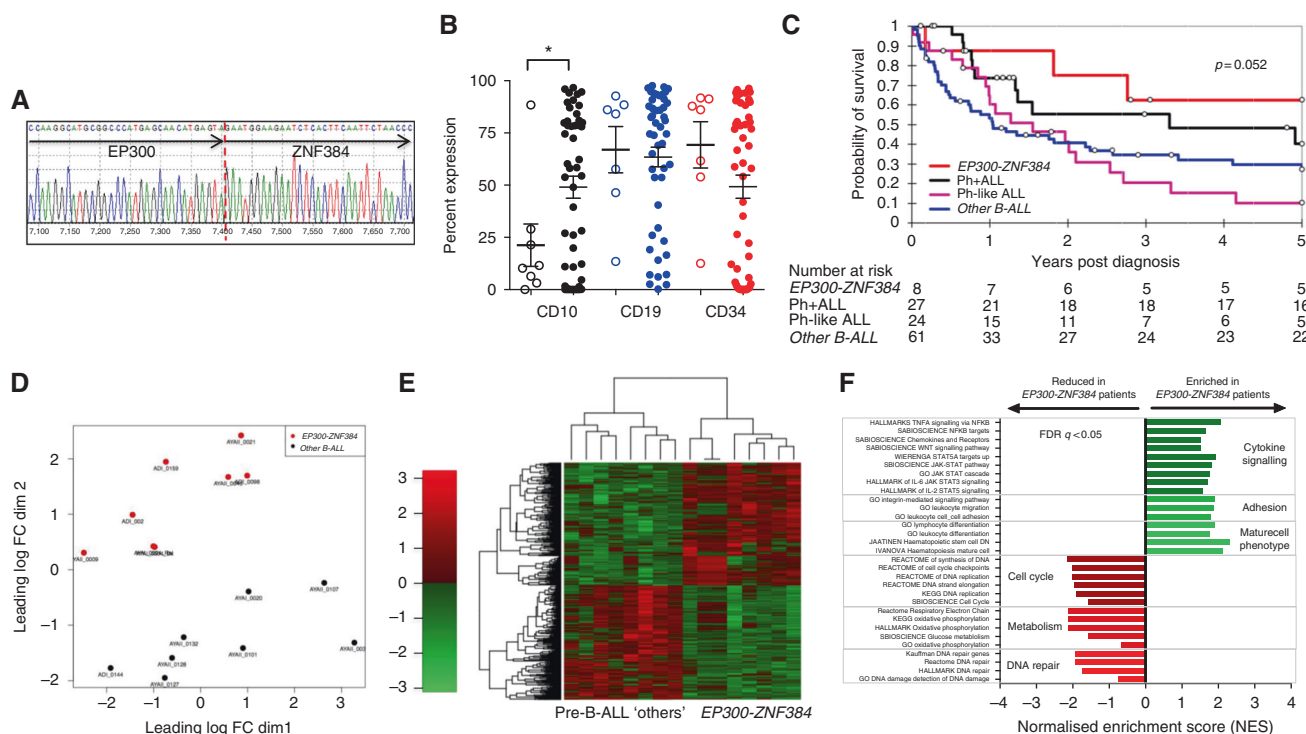


Fig. 1 Pre-B-ALL expressing EP300-ZNF384 MNC have reduced CD10 expression and a distinct gene signature, and patients have improved survival. **a** Sequence of the fusion breakpoint between EP300 (at 22p13.2) and ZNF384 (at 12p13). **b** Surface expression of CD10, CD19 and CD34 on AYA/adult MNC compared between pre-B-ALL containing EP300-ZNF384 fusion (open circles) to those without detectable EP300-ZNF384 fusions, pre-B-ALL 'others' (closed circles) * $p = 0.046$. Mean \pm SEM is shown and analysed by unpaired t -test with two-tail test. **c** Kaplan–Meier analysis of percent overall survival from diagnosis for patients classified into different subtypes; EP300-ZNF384, $n = 8$ (red), B-ALL 'other', $n = 61$ (blue), BCR-ABL1, $n = 27$ (black) and Ph-like, $n = 24$ (purple). **d** Unsupervised clustering using multidimensional scaling (MDS) plots of log-CPM values based on dimensions 1 and 2 reveals differences in gene expression from 8 AYA/adult cases containing the EP300-ZNF384 fusion (red) and 8 AYA/adult pre-B-ALL 'other' cases without detectable fusions (black) matched for age, initial white cell count (WCC) and sex (outlined in Supplementary Table 2). The distances that display on the plot correspond to the average (root-mean-square) fold-change in log₂ scale for 500 genes with the most divergent between each pair of samples by default. An interactive MDS plot of this dataset can be found at the Supplementary Figure 1. **e** Differential gene expression in AYA/adult pre-B-ALL containing EP300-ZNF384 fusion (red, $n = 8$) compared to those without detectable gene fusions (black, $n = 8$). Heatmap showing the top 100 genes with significant expression differences based on FDR $p < 0.05$. An interactive gene expression plot of this data set is available at https://github.com/chungkok/EP300_ZNF384. **f** Gene set enrichment profiling of transcriptomic sequencing data of EP300-ZNF384 ($n = 8$) versus pre-B-ALL 'other' ($n = 8$) FDR $q < 0.05$. Statistical analysis was performed in GraphPad Prism (GraphPad Software Inc., La Jolla, CA, USA)

DISCUSSION

In contrast to other reports where ZNF384 fusions have multiple 5' partners, we exclusively detected EP300-ZNF384 fusions in 5.7% of BCR-ABL1-negative AYA/adult pre-B-ALL, making it one of the more prevalent recurrent lesions in this age group. Our EP300-ZNF384 patients cluster in the AYA range and have reduced CD10 surface expression and up-regulated CD33 expression in common with previous reports.^{3,5} The EP300-ZNF384 subgroup showed improved outcome compared to other pre-B-ALL patients studied, and concurs with a Japanese cohort where ZNF384 fusions have better survival outcomes than Ph-like ALL in AYA.³ This report contributes to a better overview of the incidence of EP300-ZNF384 patients and the prognostic significance of ZNF384 lesions deserves further study and validation. Importantly, we show here that the concurrent reduction in DNA repair capacity and activation of JAK-STAT pathways and B-cell regulators appear to be the hallmark features of the pre-B-ALL subtype expressing EP300-ZNF384.

ACKNOWLEDGEMENTS

This work is supported in part by grants from National Health and Medical Research Council (NHMRC) (APP1057746, APP1044884), Australian Genomics Health Alliance (AGHA) Beat Cancer, the Leukaemia Foundation and Bristol-Meyers Squibb Company (to D.L.W.); Channel 7 Children's Research Foundation (CRF) (to S.L.H.) and

Contributing Haematologist Committee (CHC) (to D.Y.). Cytogenetic analysis was performed by Genetics and Molecular Pathology, SA Pathology, Adelaide, SA, Australia.

AUTHOR CONTRIBUTIONS

B.J.M. performed experiments, analysed the data and wrote the manuscript. S.L.H. designed and performed experiments, analysed data, proofread manuscript. C.H.K. performed cluster analysis, gene set enrichment analysis and generated heat map from transcriptomic sequencing data. T.S. performed the experiments and proofread manuscript. J.A. assessed gene transcription levels. D.Y., R.S. and R.B.L. provided patient samples and critically appraised manuscript. T.P.H. critically appraised manuscript. D.L.W. designed experiments, analysed data, proofread manuscript and supervised the project.

ADDITIONAL INFORMATION

Supplementary information is available for this paper at <https://doi.org/10.1038/s41416-018-0022-0>.

Conflict of interest: D.L.W. receives research support from Novartis and BMS, and Honoraria from BMS. T.P.H. and D.Y. receive research support from Novartis, Ariad and BMS, and Honoraria and Advisory role from Novartis. All the other authors declare that they have no conflict of interest.

Note: This work is published under the standard license to publish agreement. After 12 months the work will become freely available and the license terms will switch to a Creative Commons Attribution 4.0 International licence (CC BY 4.0).

REFERENCES

1. Mullighan, C. G. Genomic characterization of childhood acute lymphoblastic leukemia. *Semin. Hematol.* **50**, 314–324 (2013).
2. Pui, C. H. et al. A revised definition for cure of childhood acute lymphoblastic leukemia. *Leukemia* **28**, 2336–2343 (2014).
3. Yasuda, T. et al. Recurrent DUX4 fusions in B cell acute lymphoblastic leukemia of adolescents and young adults. *Nat. Genet.* **48**, 569–574 (2016).
4. Lilljebjorn, H. et al. Identification of ETV6-RUNX1-like and DUX4-rearranged subtypes in paediatric B-cell precursor acute lymphoblastic leukaemia. *Nat. Commun.* **7**, 11790 (2016).
5. Gocho, Y. et al., Tokyo Children's Cancer Study, G. A novel recurrent EP300-ZNF384 gene fusion in B-cell precursor acute lymphoblastic leukemia. *Leukemia* **29**, 2445–2448 (2015).
6. Liu, Y. F. et al. Genomic profiling of adult and pediatric B-cell acute lymphoblastic leukemia. *EbioMedicine* **8**, 173–183 (2016).
7. Dutta, R., Tiu, B. & Sakamoto, K. M. CBP/p300 acetyltransferase activity in hematologic malignancies. *Mol. Genet. Metab.* **119**, 37–43 (2016).
8. Qian, M. et al. Whole transcriptome sequencing identified a distinct subtype of acute lymphoblastic leukemia with predominant genomic abnormalities of EP300 and CREBBP. *Genome Res.* **27**, 185–195 (2017).
9. Shago, M., Ablu, O., Hitzler, J., Weitzman, S. & Abdelhaleem, M. Frequency and outcome of pediatric acute lymphoblastic leukemia with ZNF384 gene rearrangements including a novel translocation resulting in an ARID1B/ZNF384 gene fusion. *Pediatr. Blood Cancer* **63**, 1915–1921 (2016).
10. La Starza, R. et al. CIZ gene rearrangements in acute leukemia: report of a diagnostic FISH assay and clinical features of nine patients. *Leukemia* **19**, 1696–1699 (2005).
11. Hirabayashi, S. et al. ZNF384-related fusion genes consist of a subgroup with a characteristic immunophenotype in childhood B-cell precursor acute lymphoblastic leukemia. *Haematologica* **102**, 118–129 (2016).
12. Heatley, S. L. et al. High prevalence of relapse in children with Philadelphia-like acute lymphoblastic leukemia despite risk-adapted treatment. *Haematologica* **102**, e409–e493 (2017).
13. Dobin, A. et al. STAR: ultrafast universal RNA-seq aligner. *Bioinformatics* **29**, 15–21 (2013).
14. Roberts, K. G. et al. High frequency and poor outcome of Philadelphia chromosome-like acute lymphoblastic leukemia in adults. *J. Clin. Oncol.* **35**, 394–401 (2017).
15. Evans, P. M. et al. Kruppel-like factor 4 is acetylated by p300 and regulates gene transcription via modulation of histone acetylation. *J. Biol. Chem.* **282**, 33994–34002 (2007).
16. Iyer, N. G. et al. p300 regulates p53-dependent apoptosis after DNA damage in colorectal cancer cells by modulation of PUMA/p21 levels. *Proc. Natl. Acad. Sci. USA* **101**, 7386–7391 (2004).